



This is a repository copy of *Development of a high temperature material model for grade s275jr steel*.

White Rose Research Online URL for this paper:
<http://eprints.whiterose.ac.uk/118368/>

Version: Accepted Version

Article:

Toric, N., Brnic, J., Boko, I. et al. (3 more authors) (2017) Development of a high temperature material model for grade s275jr steel. *Journal of Constructional Steel Research*, 137. pp. 161-168. ISSN 0143-974X

<https://doi.org/10.1016/j.jcsr.2017.06.020>

Article available under the terms of the CC-BY-NC-ND licence
(<https://creativecommons.org/licenses/by-nc-nd/4.0/>).

Reuse

This article is distributed under the terms of the Creative Commons Attribution-NonCommercial-NoDerivs (CC BY-NC-ND) licence. This licence only allows you to download this work and share it with others as long as you credit the authors, but you can't change the article in any way or use it commercially. More information and the full terms of the licence here: <https://creativecommons.org/licenses/>

Takedown

If you consider content in White Rose Research Online to be in breach of UK law, please notify us by emailing eprints@whiterose.ac.uk including the URL of the record and the reason for the withdrawal request.



eprints@whiterose.ac.uk
<https://eprints.whiterose.ac.uk/>

DEVELOPMENT OF A HIGH TEMPERATURE MATERIAL MODEL FOR GRADE S275JR STEEL

Neno Torić^{1*}, Josip Brnić², Ivica Boko¹, Marino Brčić², Ian W. Burgess³, Ivana Uzelac Glavinic¹

Abstract:

The paper presents test results for the mechanical and creep properties of the European steel grade S275JR at high temperatures. The objective of the research was to obtain a reliable estimate of creep strain development in the temperature range 400-600°C, and to identify the critical thermo-mechanical parameters which activate the creep mechanism. Tests of mechanical properties at temperature levels up to 600°C have shown good agreement with the reduction factors for yield strength and modulus of elasticity given in Eurocode 3 and other comparable studies. A critical temperature for creep development of approximately 400°C was identified in the tests. The creep tests conducted have also shown that the creep strain rate starts to develop significantly at temperatures around 500°C when coupons are exposed to a mid-range stress level equal to 60% of the stress at 0.2% strain. The temperature level of 600°C is identified as the upper-bound temperature for creep development, since creep develops very rapidly, even at very low stress levels. Finally, the paper presents an analytical creep model suitable for implementation in Finite Element-based numerical models.

Keywords:

Steel, fire, coupon testing, mechanical properties, creep

¹ University of Split, Faculty of Civil Engineering, Architecture and Geodesy, Matice Hrvatske 15, 21000 Split, Croatia, Tel: +385-21-303-366, Fax: +385-21-303-331

* E-mail: neno.toric@gradst.hr (corresponding author)

² University of Rijeka, Faculty of Engineering, Vukovarska 58, 51000 Rijeka, Croatia

³ University of Sheffield, Department of Civil and Structural Engineering, Sir Frederick Mappin Building, Mappin Street, Sheffield, S1 3JD, UK.

1. INTRODUCTION

1.1 Motivation

Grade S275JR is currently widely used in the construction industry across Europe, as a standard grade for design of residential and industrial buildings. The mechanical properties of this steel grade at normal and elevated temperatures, for application in structural engineering design, are provided in Eurocode 3 [1] with the help of temperature-dependent reduction factors for yield strength and modulus of elasticity. Furthermore, Eurocode 3 provides a specific type of stress-strain model for Grade S275JR, which originated in a set of transient coupon tests conducted at a heating rate of 10°C/min by Kirby et al. [2-3]. These studies also served as the main source for the derivation of the reduction factors for yield strength and modulus which are implemented in Eurocode 3. The stress-strain model from Eurocode 3 contains an implicit creep strain component whose level corresponds to the heating rate used in the original tests. This type of stress-strain model is considered in Eurocode 3 Part 1-2 (Section 4.3.3, clause 4) to take into account all practical effects of thermal creep under transient heating.

Recent research [4-5], focusing on the influence of creep on the response of steel structures, has pointed out that the Eurocode 3 model has certain limitations in predicting structural response when the structure is exposed to heating rates below 10°C/min. These limitations affect estimates of deflection and determination of the fire resistance of steel members exposed to bending or eccentric load arrangements. A similar conclusion was put forward in a study conducted by Torić et al. [6] in which numerical analysis of a series of stationary fire tests on partially heated beams was conducted. The beams were loaded for a prolonged time period and heated to constant temperatures up to 700°C, which ultimately caused significant creep development in the beams.

The test methodology used for deriving the Eurocode 3 stress-strain model for Grade S275 (and other carbon steel grades such as S235 and S355) has left open questions about the adequacy of the stress-strain model to cover all possible stationary and transient

heating scenarios, including consideration of the realistic creep development which can occur during typical times of exposure to fire temperatures. Another important issue when using the Eurocode 3 stress-strain model is the inevitable doubling of creep consideration when an explicit creep analysis is attempted.

Since a proper explicit creep analysis is not possible using the Eurocode 3 material model, due to its inherent implicit creep content, a methodology for extracting the implicit creep content from the Eurocode 3 stress-strain model has recently been developed by Torić et al. [7]; this resulted in a proposal for a new type of creep-free EC3 stress-strain model [5]. The proposed stress-strain model is based on modifying the yield strain value from 2% to 1% for all temperature levels. The application of this creep-free model has been presented in a recent study [8], defining a unified rheological model for steel at high temperature which takes into account the effects of change of temperature and strain rate on the stress-strain curve of the material.

The only previous research data regarding creep behaviour of Grade S275 available in literature is given in a study by Brnić et al. [9], in which a limited range of creep test data is presented in the form of an analytical creep model. Apart from one study [9], which is based on a steel alloy with very low carbon content, it seems that there is no other available research data on creep development in the high-temperature range for this grade of steel, which can be used to assess its creep properties and resilience in fire conditions. This fact represents the main motivation for conducting a new study of mechanical properties of S275JR steel at high temperatures, and especially its creep properties. Development of an explicit creep model for grade S275 is another strong motivation for this research, since there are no reliable creep models available in the scientific literature for the purpose of conducting proper explicit-creep analyses of steel structures exposed to fire.

1.2 Creep-related research

This study of the creep behaviour of a normal structural steel at high temperatures complements other research output on steel creep properties during the past five years. These studies have mainly concentrated on the specialized steel alloys used in prestressed concrete structures and for high-strength steel, with some studies focusing on steels of mid-range strength. Gales et al. [10] investigated the creep behaviour of the BS 5896-compliant steel used in prestressing tendons for unbonded concrete structures. The testing methodology included both stationary and transient creep tests, in which strain was measured by using the Digital Image Correlation technique. The study by Wei et al. [11] was also focused on BS 5896-compliant prestressing steel, and included additional steady-state creep tests. Recent studies conducted on the Chinese grades Q345 and Q460, by Wang et al. [12-13], used a series of stationary creep tests to obtain the corresponding analytical creep model. The creep behaviour of the American steel grades A572 and A992 was recently investigated by Morovat et al. [14] and by Kodur and Aziz [15] with the help of stationary creep tests. Inspection of these recent studies shows that most of them (except study [10] in which transient tests were conducted) have relied on stationary creep tests, since these are more reliable in terms of measurements and results. Their main outputs have either been the development of various types of analytical creep model, or modification of the creep model defined by Harmathy [16].

2. TEST STUDY AND COMPARISON OF RESULTS

2.1 Test setup and methodology

The test study presented has been performed entirely at the University of Rijeka's Department of Engineering Mechanics. The test equipment and the coupon geometry are presented in Figure 1; the test equipment comprises a Zwick-Roell tensile testing machine with the maximum load capacity of 400 kN, a mobile furnace capable of heating coupons to 900°C and a high-temperature-resistant extensometer. The tested coupons were manufactured from the flanges of a European steel column section HE140B. These

columns are scheduled for testing during the later stages of the project for verification of the steel's creep properties. The coupons were threaded in order to attach to the platens of the testing machine.

Both constant-stress-rate and stationary creep tests, all at constant temperature, were conducted within the study. The test procedure for a constant-stress-rate test consists of three stages: pre-heating, during which the coupon temperature is increased to a target temperature level at an imposed furnace heating rate of 15°C/min; soaking of the coupon to the target temperature for a time period of 30 min; loading, in which the coupon is loaded at a constant stress-rate, prescribed at 10 MPa/s. The test procedure for a stationary creep test follows a similar procedure: pre-heating to a target furnace temperature at a heating rate of 15°C/min; soaking of the coupon to the target temperature for a time period of 60 min; loading, in which the coupon is loaded quickly and held at constant stress for a prolonged time period. During the loading stage for both types of test the temperature in the furnace is kept constant.

The coupon shape and geometry, including the loading arrangements, was in accordance with the guidelines of ASTM:E8M-11 [17] for ambient-temperature tests and ASTM:E21-09 [18] for high-temperature tests. A summary of the test parameters for both test types, including the test results, is presented in Tables 1 and 2. Table 3 presents a comparison of the reduction factors for yield strength at 0.2% and 2% strain, and for modulus of elasticity, between the test results and other selected studies. The test temperature range for derivation of creep properties was 400-600°C, the objective being to determine the critical temperature beyond which significant creep starts to develop (“the insignificant creep temperature”) and to cover a temperature range in which carbon steels’ mechanical properties experience significant reduction. In these investigations engineering stress-strain curves were generated at ambient temperature and at different elevated temperatures. At each temperature, before performing the full tensile test, the modulus of elasticity was first determined. Determination of a modulus of elasticity was based on an average from 5-10 tensile tests carried out on the same specimen in the elastic domain. These test results are provided automatically by the computer-controlled testing machine and are based on a regression method.

2.2 Test studies for comparison

In order to compare the tested mechanical and creep properties of S275JR steel, several compatible test studies have been chosen. As previously mentioned, a study by Brnić et al. [9] was selected for comparison, since it is based on tests of a S275JR alloy. A study by Kirby and Preston [2] was selected, since its test results represent the main background for the creation of the Eurocode 3 material model and its corresponding reduction factors. The difference between the authors' study and the latter is that the stress-strain curves from Kirby and Preston were determined by means of transient coupon tests heated at 10°C/min on the now-superseded steel Grade 43A with an ambient-temperature yield strength of approximately 267 MPa, which is close to the yield strength of the tested grade. Results from studies by Harmathy [16, 19], and the corresponding creep model, were selected for comparison with the creep tests conducted, although the material creep parameters are based on the American A36 grade. However, the chemical composition and the yield strength value (approximately 306 MPa [19]) of this particular alloy are similar to those of the tested S275JR alloy. The nominal mechanical properties from Eurocode 3 were also used for comparison. The chemical compositions of these steels are presented in Table 4. It can be seen that the studied alloy has a carbon content similar to the others, with the exception of Brnić's study [9] which used steel with a lower carbon content.

Four other previous studies were also used for the purpose of comparison. The study by Latham and Kirby [20] was selected since it is based on stationary strain-rate tests of Grade S275 steel. The results of a test at a moderate strain-rate of 0.02min⁻¹ have been chosen for comparison. A new NIST material model [21] was also selected, since it is partially calibrated using currently available S275 properties data; the parameters for ordinary steel were chosen for comparison. Work by Boko et al. [22] based on S355 steel was selected for comparison of the reduction factors for yield strength and modulus of elasticity; these were determined using constant-strain-rate tests at 0.0002s⁻¹, which is comparable with the Latham and Kirby study. Finally, tests by Renner [23] at moderate strain rates were selected, since they focus on yield strength reduction factors at 2% strain for Grade S275 steel.

2.3 Test results and comparison

Figure 2(a) presents the engineering stress-strain curves obtained from the constant stress-rate tests. Figures 2(b-e) respectively present comparisons of the stress-strain curves obtained against the Eurocode 3 creep-free material model [5], Latham and Kirby [20], Kirby and Preston [2] and the NIST model [21]. A further comparison of test results against Brnić et al. [9] is presented in Figure 3(a), and the test reduction factors for yield strength and modulus of elasticity are compared with other studies in Figures 3(b-d). Figure 4 shows similar output from the stationary creep test series in the temperature range 400-600°C. Figure 5 presents a comparison between the creep tests at 400°C and predictions from the research software Vulcan [24] using Harmathy's explicit creep model [16]. It is important to note that the original Harmathy creep model is capable of taking into account only the primary and secondary creep phases. However, it can be noted that the tertiary creep phase can be represented with the Harmathy model only if the geometrical changes of the coupon are measured during the test, by applying the experimental procedure explained in reference [10]. Since the conducted tests were based on measurements of the deformation of a coupon as whole, the recorded strain output in the tertiary creep phase can be considered as an averaged version of tertiary creep, since tertiary creep strain exhibits higher values within the necking region [10]. Harmathy's creep model uses the following equations for creep strains:

$$\varepsilon_{cr} = \frac{\varepsilon_{cr,0}}{0.693} \cdot \cosh^{-1} \left(2^{\frac{\theta}{\theta_0}} \right) \quad (\theta < \theta_0) \quad (1)$$

$$\varepsilon_{cr} = \varepsilon_{cr,0} + Z\theta \quad (\theta \geq \theta_0) \quad (2)$$

$$\theta_0 = \varepsilon_{cr,0} / Z \quad (3)$$

$$\theta = \int_0^t \exp^{\frac{-\Delta H}{RT_R}} dt \quad (4)$$

in which T_R is the temperature (°K), R is the universal gas constant (J/mol °K), ΔH is the creep activation energy (J/mol), Z is the Zener-Hollomon parameter (h^{-1}), $\varepsilon_{cr,0}$ is a dimensionless creep parameter, t is time, and θ represents temperature-compensated time.

The material parameters Z , $\Delta H/R$ and $\varepsilon_{cr,0}$ for this model can be found in [19]. The parameters for the American steel A36 from study [19] are subsequently used for comparison of the performance of the Harmathy model with the analytical model developed in this paper.

The inclusion of creep strain into structural modelling can be achieved through explicit consideration of creep strain in the total strain equation [25]:

$$\varepsilon_{tot} = \varepsilon_{th}(T) + \varepsilon_{\sigma}(\sigma, T) + \varepsilon_{cr}(\sigma, T, t) \quad (5)$$

In which: ε_{tot} is the total strain, $\varepsilon_{th}(T)$ is the temperature-dependent thermal strain and $\varepsilon_{\sigma}(\sigma, T)$ is the stress-related strain, which depends upon the applied stress σ and temperature T . The strain $\varepsilon_{cr}(\sigma, T, t)$ is the stress-, temperature- and time-dependent creep strain. It is important to note that in this analysis the stress-related strain represents a creep-free strain which is based on the creep-free model developed in [5]. The constitutive stress-strain relationship of the creep-free model is given by the following expressions:

$$\sigma = \varepsilon E_{a,0} \quad (\text{for } \varepsilon \leq \varepsilon_{p,0}) \quad (6)$$

$$\sigma = f_{p,0} - c + (b/a) \left[a^2 - (\varepsilon_{y,0} - \varepsilon)^2 \right]^{0.5} \quad (\text{for } \varepsilon_{p,0} < \varepsilon < \varepsilon_{y,0}) \quad (7)$$

$$\sigma = f_{y,0} \quad (\text{for } \varepsilon_{y,0} < \varepsilon < 0.04) \quad (8)$$

Parameters a^2 , b^2 and c are defined as follows:

$$\begin{aligned} a^2 &= (\varepsilon_{y,0} - \varepsilon_{p,0})(\varepsilon_{y,0} - \varepsilon_{p,0} + c/E_{a,0}) \\ b^2 &= c(\varepsilon_{y,0} - \varepsilon_{p,0})E_{a,0} + c^2 \\ c &= \frac{(f_{y,0} - f_{p,0})^2}{(\varepsilon_{y,0} - \varepsilon_{p,0})E_{a,0} - 2(f_{y,0} - f_{p,0})} \end{aligned} \quad (9)$$

in which $\varepsilon_{p,0} = f_{p,0}/E_{a,0}$ and $\varepsilon_{y,0} = 0.01$, which represents a modified value of the nominal yield strain, used to exclude implicit creep. The parameters $f_{p,0}$, $f_{y,0}$, $E_{a,0}$ respectively represent the proportional limit, yield strength and modulus of elasticity at temperature θ .

Modelling of the coupon tests was conducted by using two three-noded line elements with appropriate segmentation of the cross-section as an 8x8 matrix.

2.4 Analytical creep model

The creep test results presented in Figure 4 were used as the background for an analytical creep model. This was created in order to convert the test results to a more general form, which allows the creep model to be implemented in numerical modelling software based on the Finite Element Method. The developed analytical model is capable of representing the test results within each of the primary, secondary and tertiary creep phases. The model is defined with the help of a polynomial function:

$$\varepsilon(\sigma, T, t) = \varepsilon_{el} + \varepsilon_{cr} = c + a \cdot t^b + e \cdot t^f \quad (10)$$

in which: ε_{el} is the elastic strain, ε_{cr} is the creep strain (%), t is time (min) and

$\varepsilon_{el} = c = \frac{\sigma}{E_{y,\theta}} \cdot 100$. The coefficients a , b , e and f are determined by curve-fitting of the

creep test results for various stress levels (Figure 4), while the value of the coefficient c represents the elastic strain which can easily be obtained by dividing the initial stress level by the temperature-dependent modulus of elasticity $E_{y,\theta}$. The coefficients used in Equation (10) are presented in Table 5. The analytical model can also be utilized to interpolate a creep curve for the intermediate stress levels at the temperatures which were used in the tests.

Figure 6(a) presents a comparison between the proposed analytical creep model and the results obtained from the creep tests at 500°C. It can be seen that Equation (10) is in good agreement with the experimental results for steel grade S275JR for this temperature level, and for all three distinct creep phases. Figure 6(b) presents a comparison between the test results at the intermediate temperature levels of 450°C and 550°C and the predictions of the analytical model. The plot of the creep output using this creep model is based on linear interpolation at a test stress ratio of $\sigma/f_{0.2,\theta}$ and temperatures of 400°C, 500°C and 600°C. The comparison shown in Figure 6(b) indicates that the linear interpolation scheme

using the stress ratio $\sigma / f_{0.2,\theta}$ provides a conservative prediction of the creep evolution at intermediate temperature levels.

2.5 Microstructure of steel

Figure 7 presents a photograph of the steel's microstructure obtained from optical microscopy at 200x magnification. The structure shows ferrite and pearlite with a distinct strip-like structure pattern which is characteristic of the low-carbon steels used in hot-rolled profiles. Since the temperature range used was below 600°C, no change in the microstructure was observed compared to that of unheated specimens. Vickers hardness tests were conducted for specimens at 20°C and 600°C, and these showed an increase in hardness value from 131.6 at 20°C to 173.6 at 600°C.

3. DISCUSSION OF THE RESULTS

3.1 Stress-strain curves

Figure 2(b) shows that the test results from constant-stress-rate tests are very similar to the newly-proposed creep-free Eurocode 3 model [5], which provides support for the objective of creating this model. Eurocode 3 proposes a stress-strain model whose strain output is greater than the mechanical strain usually occurring at high temperatures for grades S235, S275 and S355. If this generic form of stress-strain model is combined with an explicit creep model it is reasonable to assume that it can simulate earlier failure of structural steel members. However, in the absence of further test results, on S235 and S355, it is premature to claim that the creep model is applicable to these grades.

Comparison with study [20] indicates some discrepancy when comparing the yield strength values from this study at various temperatures with the derived stress-strain curves, which can be attributed to the different effects of strain-rate on the change of yield strength. It can be seen that the effect of increase of yield strength is not of the same order of magnitude when the results of constant stress- and strain-rate tests at the same temperature levels are compared; this is clearly illustrated in Figure 2(c).

Figure 2(d) clearly depicts the amount of implicit creep which was present in the transient-test-based stress-strain curves proposed by Kirby and Preston. Consequently, comparison of strain predictions between the constant-stress-rate and transient test curves show discrepancies within the entire strain range. Comparison with the NIST model [21] from Figure 2(e) shows a certain level of discrepancy in predicting the effect of strain-rate on the increase of yield strength of S275 at high temperature. This can be attributed to the fact that the NIST model is better adjusted to representing strain-rate-controlled tests rather than stress-rate-controlled tests, since it contains an explicit strain-rate term in its constitutive model.

3.2 Mechanical properties

Figures 3(a-b) show that the test values of stress at 0.2% strain and modulus of elasticity are comparable with test results from study [9], which indicates that in general there is no substantial variation in the major mechanical properties of grade S275. The comparison shown in Figure 3(c) points to a slightly lower reduction of test yield strengths compared to the reduction factors from Eurocode 3 within the range 400°C-600°C. This observation is also apparent from the other studies which were selected for comparison. Figure 3(d) shows that the values of the reduction factors for modulus of elasticity obtained from the current test series are higher than those from Eurocode 3, and this is also seen in other comparable studies. In general terms it can be concluded that the mechanical properties obtained from this study are very close to the previous test studies, and that there are no significant variations of mechanical properties of S275 at high temperatures when comparing different studies.

3.3 Critical temperatures for creep development

Observations from Figure 4(a) indicate that the apparent insignificant creep temperature beyond which creep development accelerates is very close to 400°C. This assertion is based on observation of the primary creep phase, which develops without entering into the other two phases at high stress, and of the value of total strain after a period of 240 minutes into fire heating, which is a function of all the important material

variables. As can be observed from Figure 4(a), only the primary creep phase develops for stresses in the range given by 0.7-0.9 of the stress at 0.2% strain ($f_{0.2,\theta}$). The lower creep strain values up to 240 minutes interval (if compared to the value of mechanical yield strain for which the maximum value is of the order of 1%) in this range also suggest that the creep activation mechanisms start to occur close to 400°C for the tested steel. This observation is also in line with the results reported by study [9] regarding the initial creep development temperature for Grade S275 steel.

Test results at the intermediate temperature of 450°C (Figure 6(b)) reveal the occurrence of tertiary creep after approximately 600 minutes at stress level of 0.75 $f_{0.2,\theta}$. This cannot be considered as a temperature at which considerable creep development is occurring, since it occurs after a time which is much longer than the duration of a general building fire (generally considered as within four hours). At 500°C (Figure 4(b)) a noticeable increase in creep strain development occurs in the stress range 0.5-0.8 $f_{0.2,\theta}$, which covers the normal utilization factor of columns in structural systems.

Figure 4(c) shows the occurrence of the tertiary creep phase in the very low stress-level range between 0.25-0.3 $f_{0.2,\theta}$. This result can be interpreted as a good estimate of the ultimate critical temperature for creep development, since it points to a temperature value at which creep develops at very low stress level. The fast occurrence of tertiary creep at lower stress levels for the same temperature was also observed in study [9] when comparing quantitative creep values.

3.4 Times of occurrence of distinct creep phases

It is generally considered in structural fire modelling that only the primary and secondary creep phases matter in the context of structural failure, since the tertiary creep phase should affect only steel components with very small cross-sectional area; these are not commonly used in steel construction, except when utilizing high-strength steel in prestressed concrete. By analysing the times of occurrence of the secondary and tertiary creep phases (Figures 4 and 6) and comparing these values within a maximum fire duration of four hours, it can be seen that both the secondary and tertiary phases occur within this maximum fire duration at 500°C for all stress levels. This observation supports the claim

that, even at 500°C, low-carbon steel does not possess sufficient creep resistance. This is an important observation, since the generally-assumed critical temperature for carbon steels' mechanical properties is approximately 600°C.

3.5 Comparison with selected creep tests and models

The comparisons shown in Figure 5 indicate that Harmathy's creep model underpredicts the amount of creep strain in the primary and secondary phases at 400°C. Since all the remaining test results show a distinctive tertiary creep phase, no further comparison with Harmathy's model is made. The discrepancy between the Harmathy model and the test results can be attributed to the outdated A36 creep parameters which, combined with its untypical chemical composition, contribute to the observed discrepancy.

These observations suggest that European S275 steel exhibits higher creep strain levels than the American steel grade A36. A comparison with the published results from study [9] shows that the order of magnitude of creep strain from the authors' study and study [9] is comparable when analysing creep strains at 400°C.

4. CONCLUSION

A test study of mechanical and creep properties of grade S275JR at high temperatures is presented in this paper. The main contribution of the study is the determination of critical thermo-mechanical parameters which govern creep development in terms of initial and ultimate temperatures. The creep model for Grade S275 presented in this study represents a significant contribution, since no other explicit-creep model is currently available to the scientific community. From the results presented and their comparison with selected test studies and Eurocode 3, the following conclusions can be drawn:

- The mechanical properties given by the tests at high temperature are very similar to those from both Eurocode 3 and the selected studies, indicating negligible variability;

- Creep tests have provided a good estimate of the initial creep temperature of 400°C for the onset of creep development;
- A good estimate of the ultimate creep temperature of 600°C, at which very rapid creep strain rates occurred at the lower stress levels, was determined from the creep tests;
- The analytical model developed for Grade S275 adequately replicates the creep tests across all three distinct creep phases.

Acknowledgement

This work has been fully supported by Croatian Science Foundation under the project Influence of creep strain on the load capacity of steel and aluminium columns exposed to fire (UIP-2014-09-5711).

REFERENCES

- [1] EN 1993-1-2:2005, “Eurocode 3 – Design of steel structures – Part 1-2: General Rules – *Structural fire design*”, European Committee for Standardization, Brussels, 2005.
- [2] Kirby, B.R. and Preston, R.R., “High Temperature Properties of Hot-Rolled, Structural Steels for Use in Fire Engineering Design Studies”, *Fire Safety Journal*, 1988, 13:27-37.
- [3] Rubert, A. and Schaumann P., “Temperaturabhaengige Werkstoffeigenschaften von Baustahl bei Brandbeanspruchung”, *Stahlbau*, 1985, 3, 81-86.
- [4] Torić, N., Harapin, A. and Boko, I., “Experimental Verification of a Newly Developed Implicit Creep Model for Steel Structures Exposed to Fire”, *Engineering Structures*, 2013; 57:116-124.
- [5] Torić, N., Sun R.R. and Burgess, I.W. “Creep-free fire analysis of steel structures with Eurocode 3 material model”, *Journal of Structural Fire Engineering*, 2016; 7(3), 234-248.

- [6] Torić, N., Harapin A., Boko I.: “Modelling of the influence of creep strains on the fire response of stationary heated steel members“, *Journal of Structural Fire Engineering*, 2015; 6(3), 155-176.
- [7] Torić, N., Sun R.-R., Burgess, I.W., “Development of a creep-free stress-strain law for fire analysis of steel structures”, *Fire and Materials*, 2016; 40(7):896-912. (DOI: 10.1002/fam.2347)
- [8] Torić, N. and Burgess, I.W., “A unified rheological model for modelling steel behaviour in fire conditions”, *Journal of Constructional Steel Research*, 2016; 127:221-230. (DOI: 10.1016/j.jcsr.2016.07.031)
- [9] Brnić J., Turkalj G., Jitai N., Čanadija M., Lanc D., “Analysis of experimental data on the behavior of steel S275JR – Reliability of modern design”, *Materials and Design*, 2013; 47:497-504.
- [10] Gales J., Robertson L., Bisby L., “Creep of prestressing steels in fire”, *Fire and Materials*, 2016; 40(7):875-895.
- [11] Wei Y., Zhang L., Francis T. K. Au, Jing L., Tsang Neil C. M., “Thermal creep and relaxation of prestressing steel”, *Construction and Building Materials*, 2016; 128:118-127.
- [12] Wang W., Yan S. and Kodur V., “Temperature Induced Creep in Low-Alloy Structural Q345 Steel,” *Journal of Materials in Civil Engineering*, 2016; 28(6), DOI: 10.1061/(ASCE)MT.1943-5533.0001519
- [13] Wang W., Yan S. and Liu J., “Studies on temperature induced creep in high strength Q460steel”, *Materials and Structures*, 2017:50-68, DOI: 10.1617/s11527-016-0941-2
- [14] Morovat M. A., Lee J., Engelhardt M. D., Taleff E. M., Helwig T. A., Segrest V. A., “Creep properties of ASTM A992 steel at elevated temperatures“, *Advanced Materials Research*, 2012; 446–449:786–792.
- [15] Kodur V. K. and Aziz E. M., “Effect of temperature on creep in ASTM A572 high-strength low-alloy steels“, *Materials and Structures*, 2015, DOI: 10.1617/s11527-014-0262-2
- [16] Harmathy, T. Z., “A Comprehensive Creep Model”, *Journal of Basic Engineering*, 1967, 89(3): 496-502.
- [17] ASTM E8 / E8M-11, *Standard Test Methods for Tension Testing of Metallic Materials*, ASTM International, West Conshohocken, PA, 2011.
- [18] ASTM E21-09, *Standard Test Methods for Elevated Temperature Tension Tests of Metallic Materials*, ASTM International, West Conshohocken, PA, 2009.
- [19] Harmathy, T. Z. and Stanzak, W.W., “*Elevated-Temperature Tensile and Creep Properties of Some Structural and Prestressing Steel*”, National Research Council of Canada, Division of Building Research, Ottawa, 1970.

- [20] Latham D. and Kirby, B.R., “Elevated temperature behaviour of welded joints in structural steels”, European commission, Technical steel research-final report 1998, 58-60.
- [21] NIST Technical Note 1907, Temperature-Dependent Material Modeling for Structural Steels: Formulation and Application, National Institute of Standards and Technology, April 2016. (DOI: 10.6028/NIST.TN.1907)
- [22] Boko, I., Torić, N. and Peroš, B., “Structural fire design parameters and procedures – analysis of the potential of Eurocode 3”, *Materialwissenschaft und Werkstofftechnik*, 2012; 43(12):1036-1052.
- [23] Renner, A., *The Effect of Strain-Rate on the Elevated-Temperature Behaviour of Structural Steel*, Research dissertation, University of Sheffield, Department of Civil and Structural Engineering, 2005.
- [24] Sun R.-R., Huang Z. and Burgess I.W., “Progressive collapse analysis of steel structures under fire conditions”, *Engineering Structures*, 2012; 34:400-413.
- [25] Anderberg, Y. “Modelling Steel Behaviour”, *Fire Safety Journal*, 1988; 13(1):17-26.

Figure Captions

Figure 1: Coupon geometry and test setup

Figure 2: Stationary stress-strain curves – test results and comparison with other studies

Figure 3: Yield strength and modulus of elasticity – comparison with other studies

Figure 4: Test results of stationary creep tests 400-600°C

Figure 5: Comparison between the creep test results and comparable creep models at 400°C

Figure 6: Comparison between the proposed analytical model and experimental creep results at 450-550 °C

Figure 7: Steel's microstructure at 200x magnification

Table Captions

Table 1: Summary of test results for stationary stress-rate tests

Table 2: Summary of test results for stationary creep tests

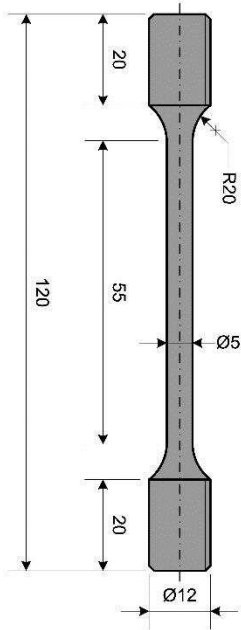
Table 3: Comparison between the test results of mechanical properties with Eurocode 3 and other studies

Table 4: Comparison of chemical composition between the studied alloy and other sources

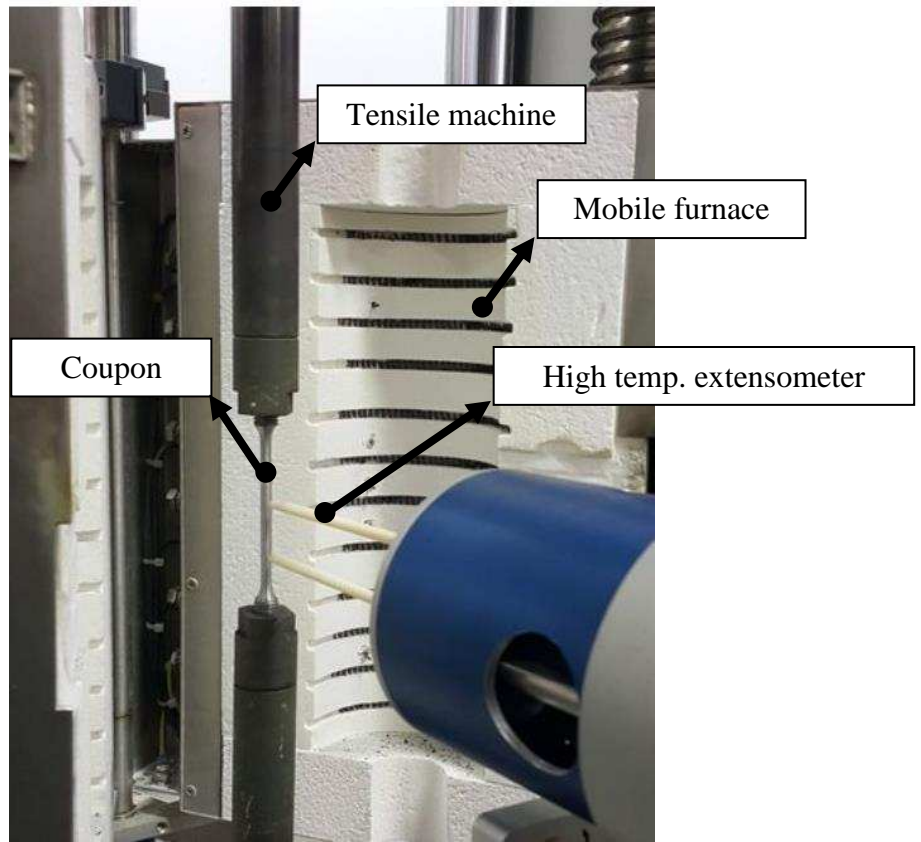
Table 5: Parameters for the developed analytical creep model

Nomenclature

$f_{y,20}$	- yield strength at normal temperature
$f_{y,\theta}$	- <i>yield strength at temperature θ</i>
$f_{0.2}$	- stress at 0.2% strain at normal temperature
$f_{0.2,\theta}$	- stress at 0.2% strain at <i>temperature θ</i>
f_u	- ultimate strength at normal temperature
$f_{u,\theta}$	- <i>ultimate strength at temperature θ</i>
$E_{y,20}$	- modulus of elasticity at normal temperature
$E_{y,\theta}$	- modulus of elasticity <i>at temperature θ</i>
$k_{E,\theta}$	- <i>reduction factor for modulus of elasticity at temperature θ</i>
$k_{y,\theta}$	- <i>reduction factor for yield strength at temperature θ</i>
ε_t	- ultimate strain

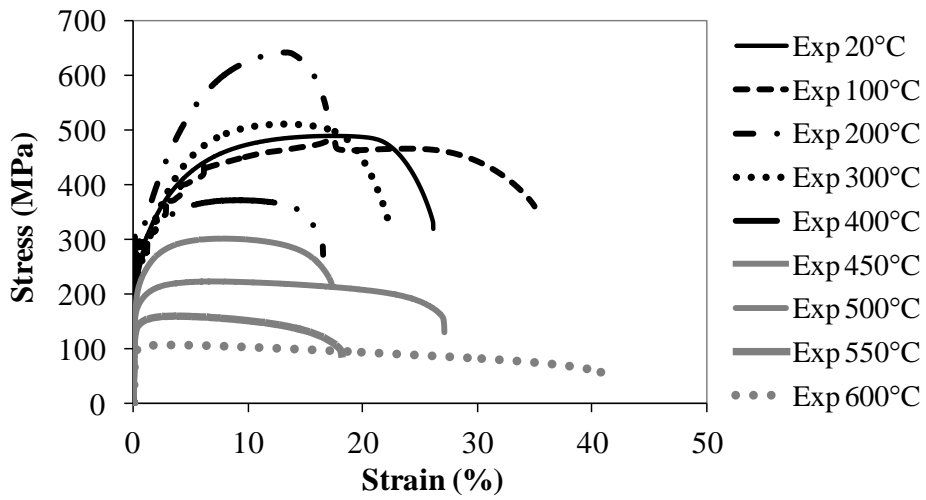


(a) Coupon geometry

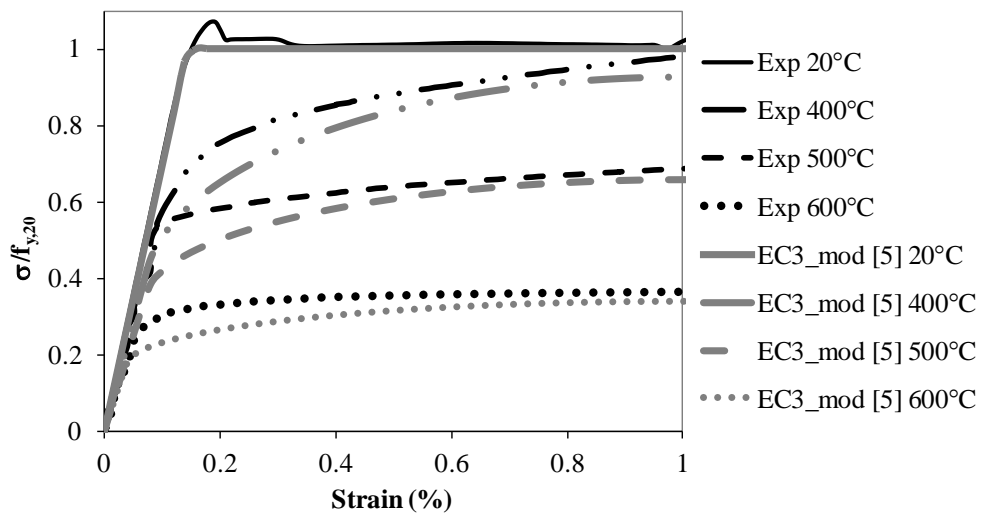


(b) Test equipment

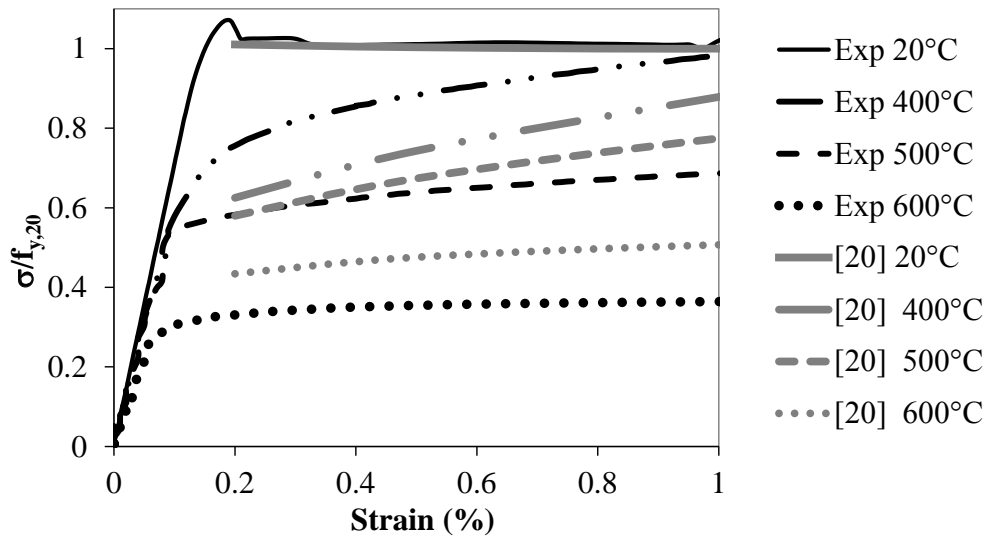
Figure 1



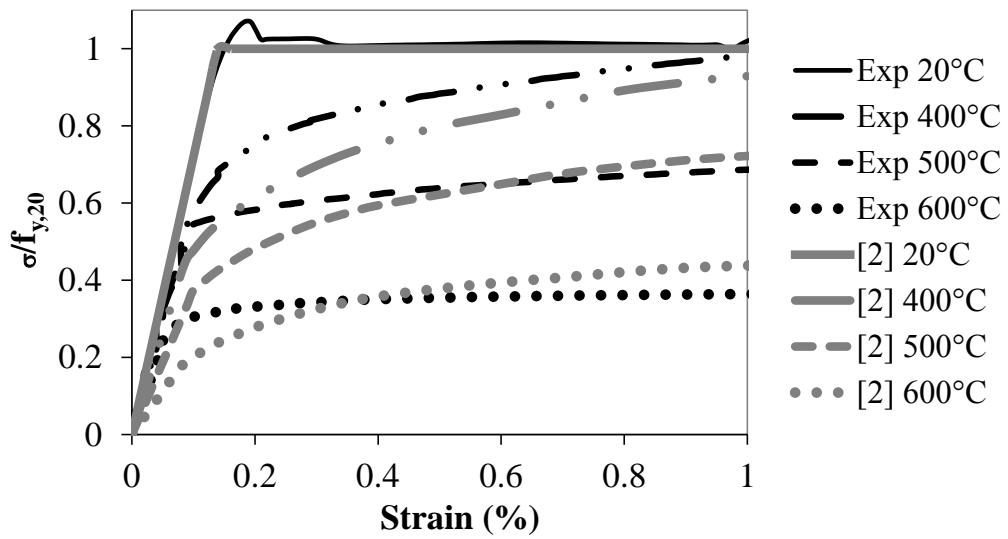
(a) Stress-strain test results



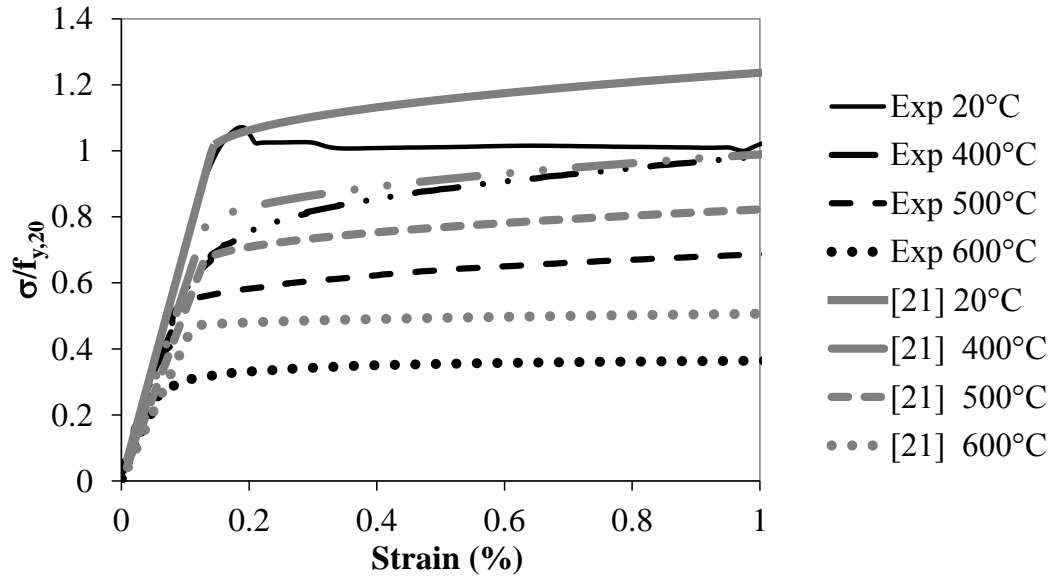
(b) Comparison with the modified EC3 creep-free model



(c) Comparison with strain-rate tests - 0.02 min^{-1} [20]

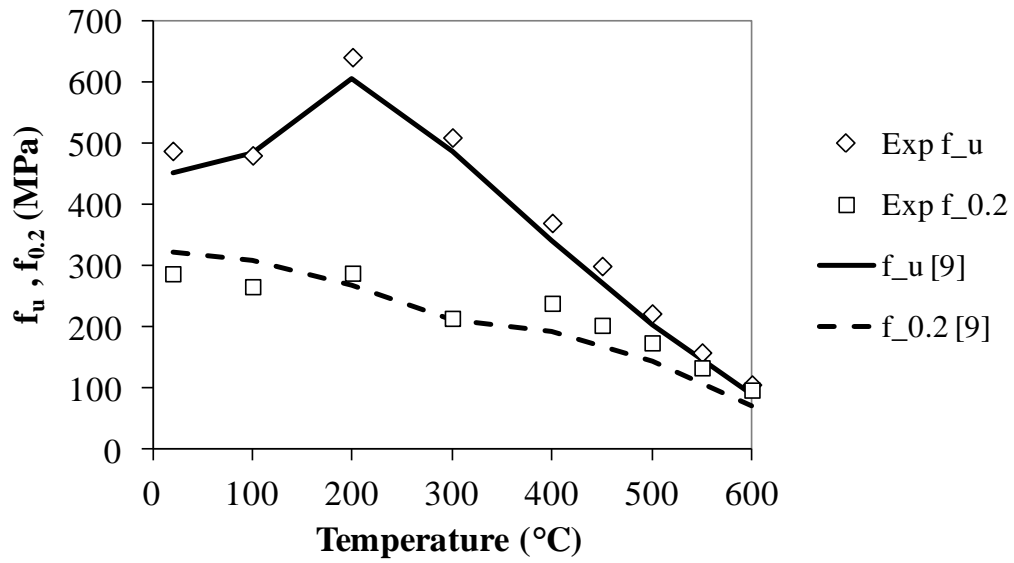


(d) Comparison with transient coupon tests - $10^\circ\text{C}/\text{min}$ [2]

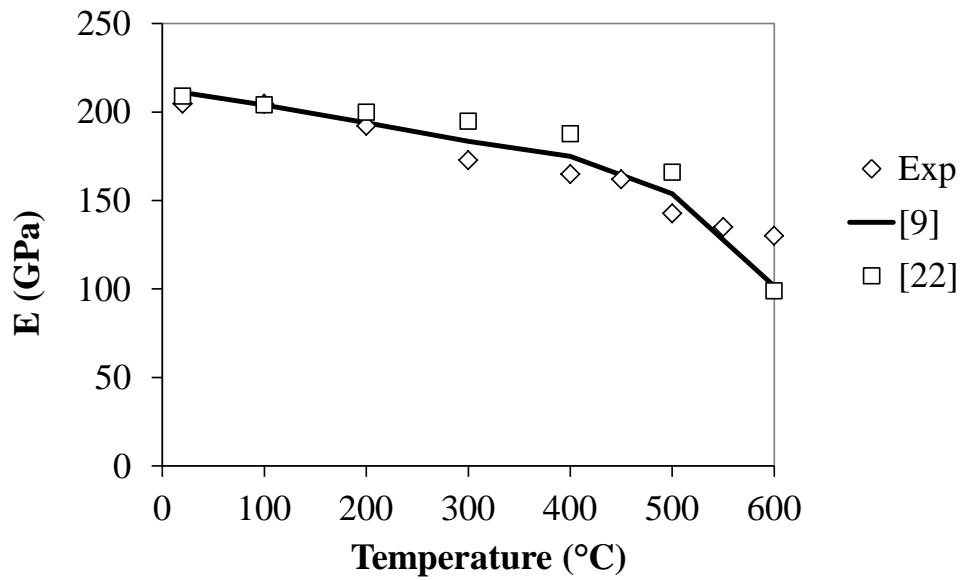


(e) Comparison with NIST stress-strain model – ordinary steel [21]

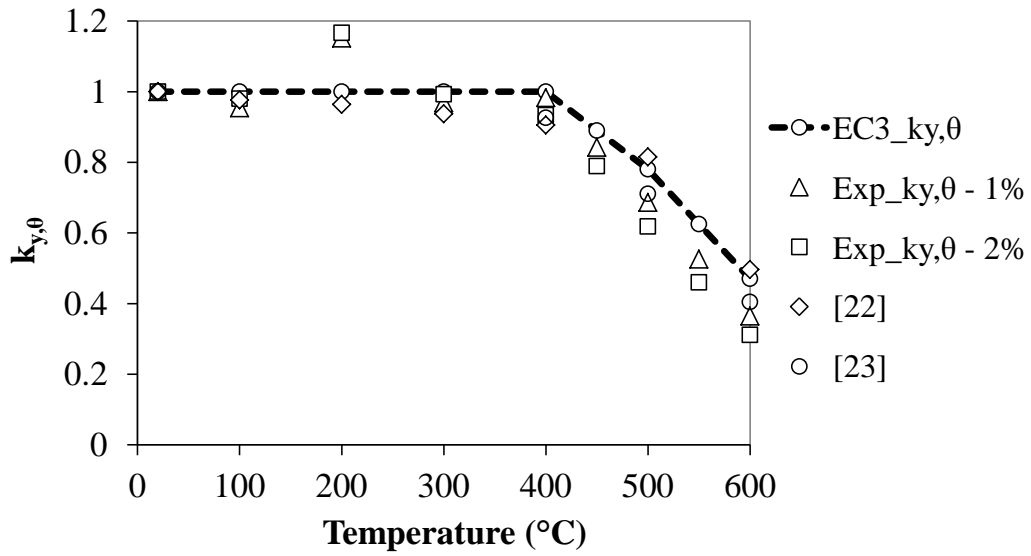
Figure 2



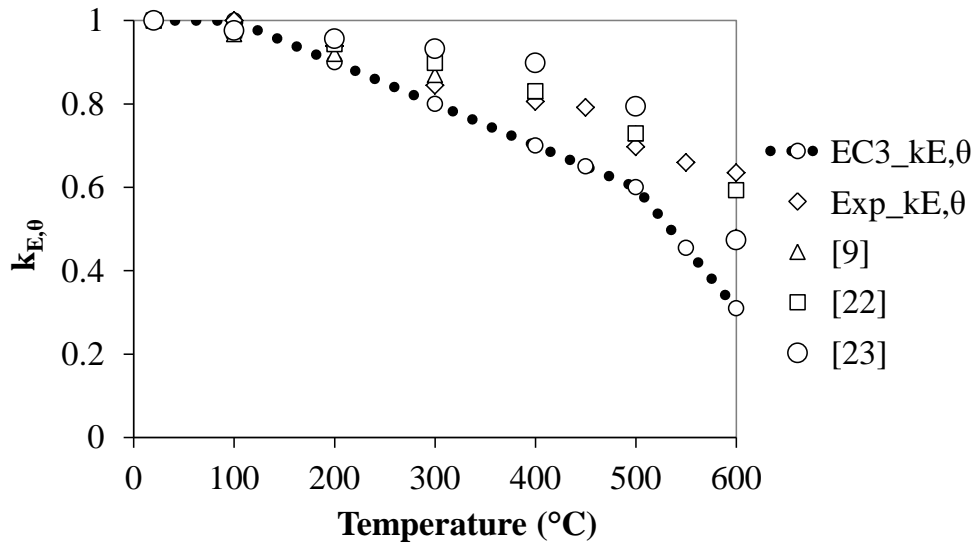
(a) Reduction of 0.2% stress and ultimate strength – comparison with study [9]



(b) Reduction of modulus and comparison with other studies

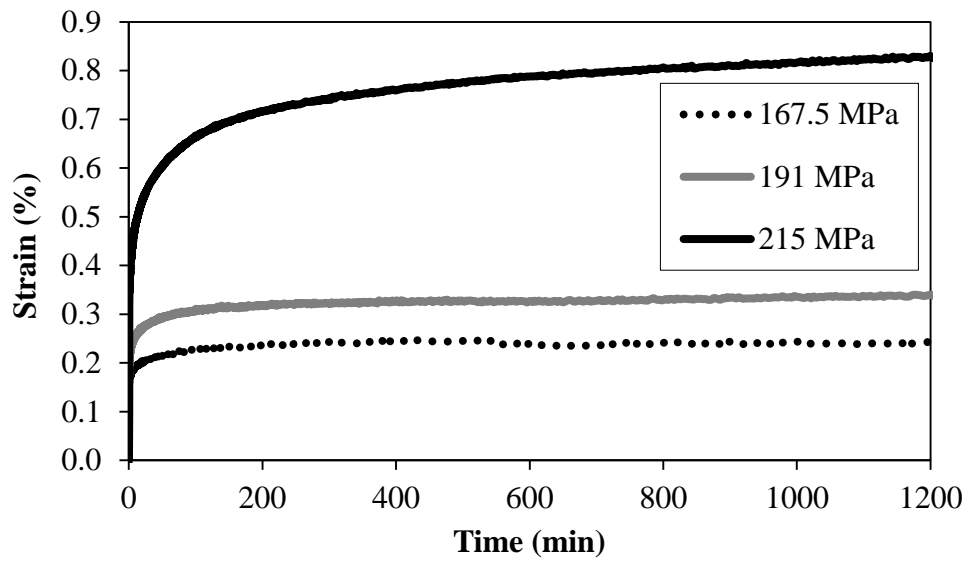


(c) Comparison of reduction factors for yield strength with other studies

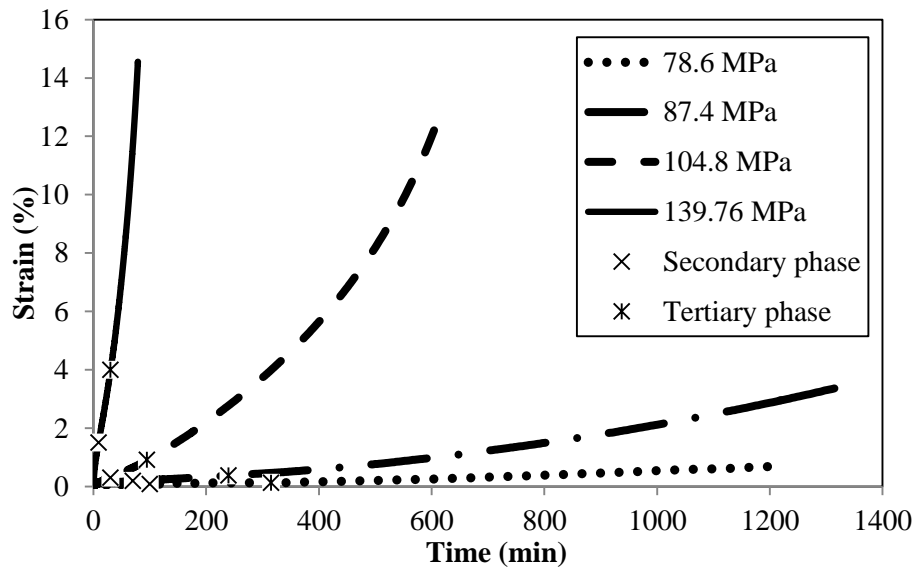


(d) Comparison of reduction factors for modulus of elasticity with other studies

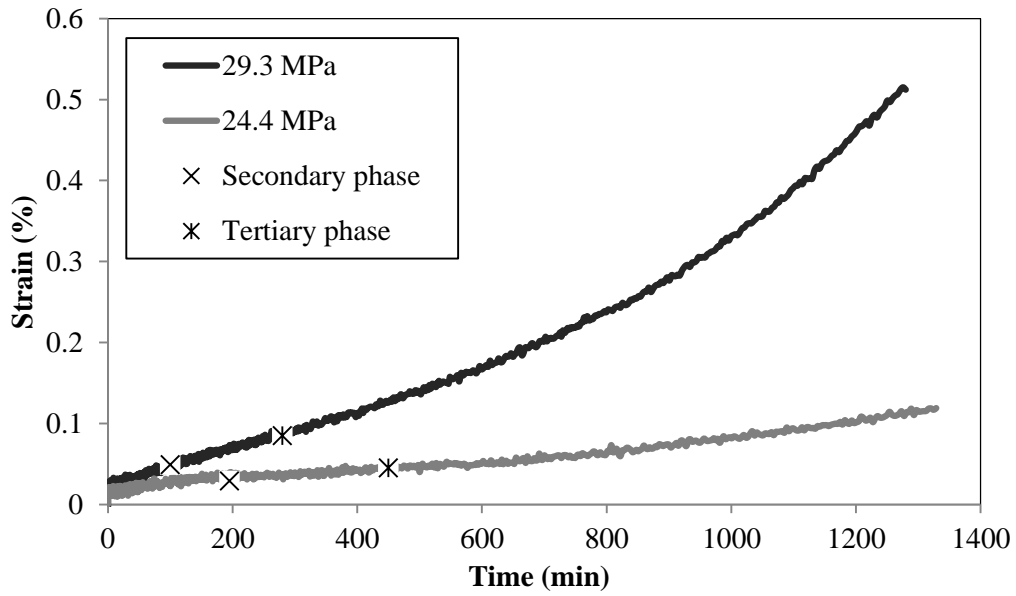
Figure 3



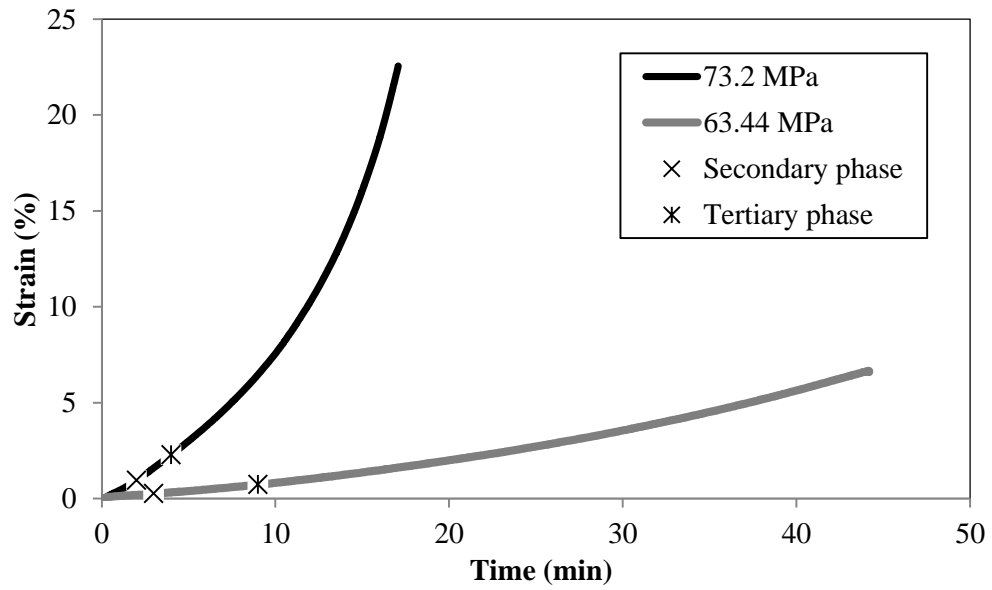
(a) Creep tests at 400°C



(b) Creep tests at 500°C



(c) Creep tests at 600°C – 0.25-0.3 $\sigma_{0.2}$



(d) Creep tests at 600°C – 0.65-0.75 $\sigma_{0.2}$

Figure 4

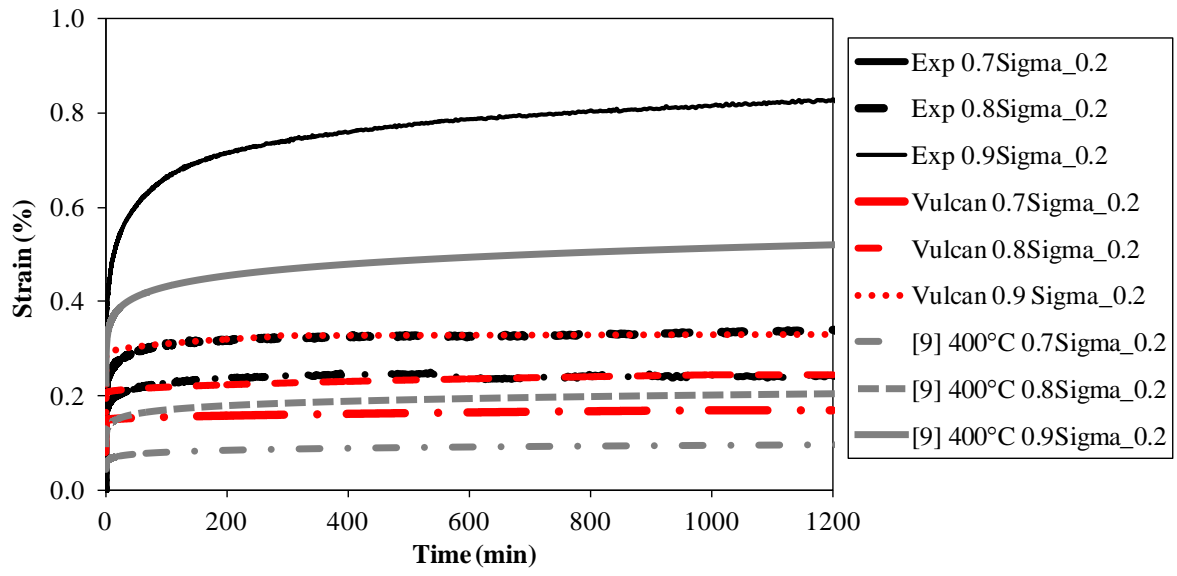
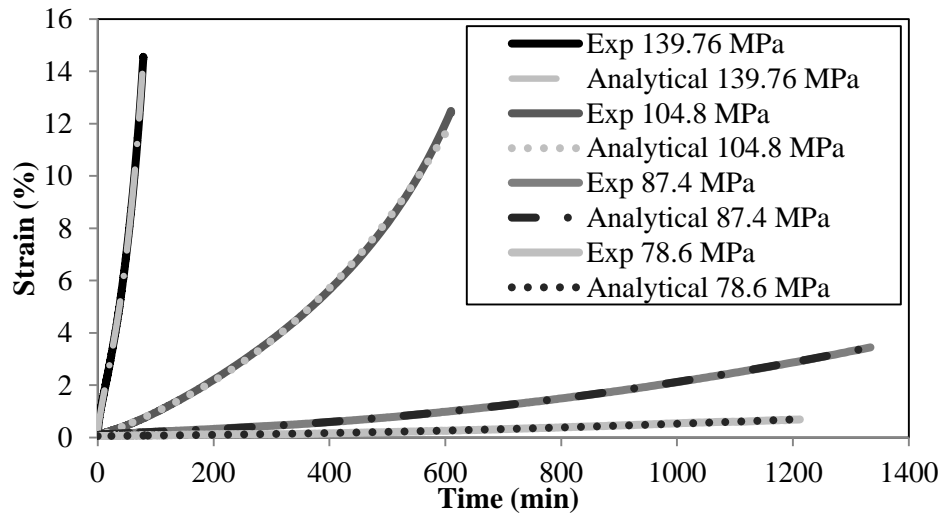
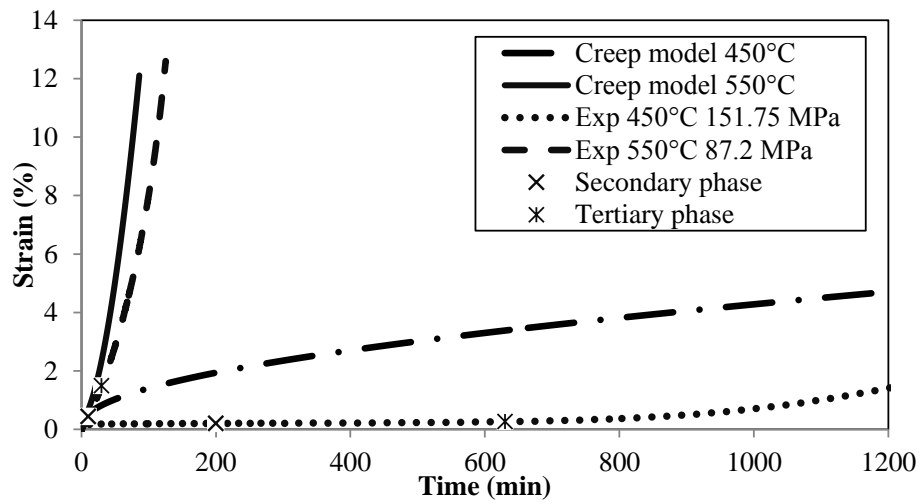


Figure 5



(a) Comparison between the analytical model and creep test results – 500°C



(b) Comparison between the analytical model and the creep test results at 450 and 550°C

Figure 6

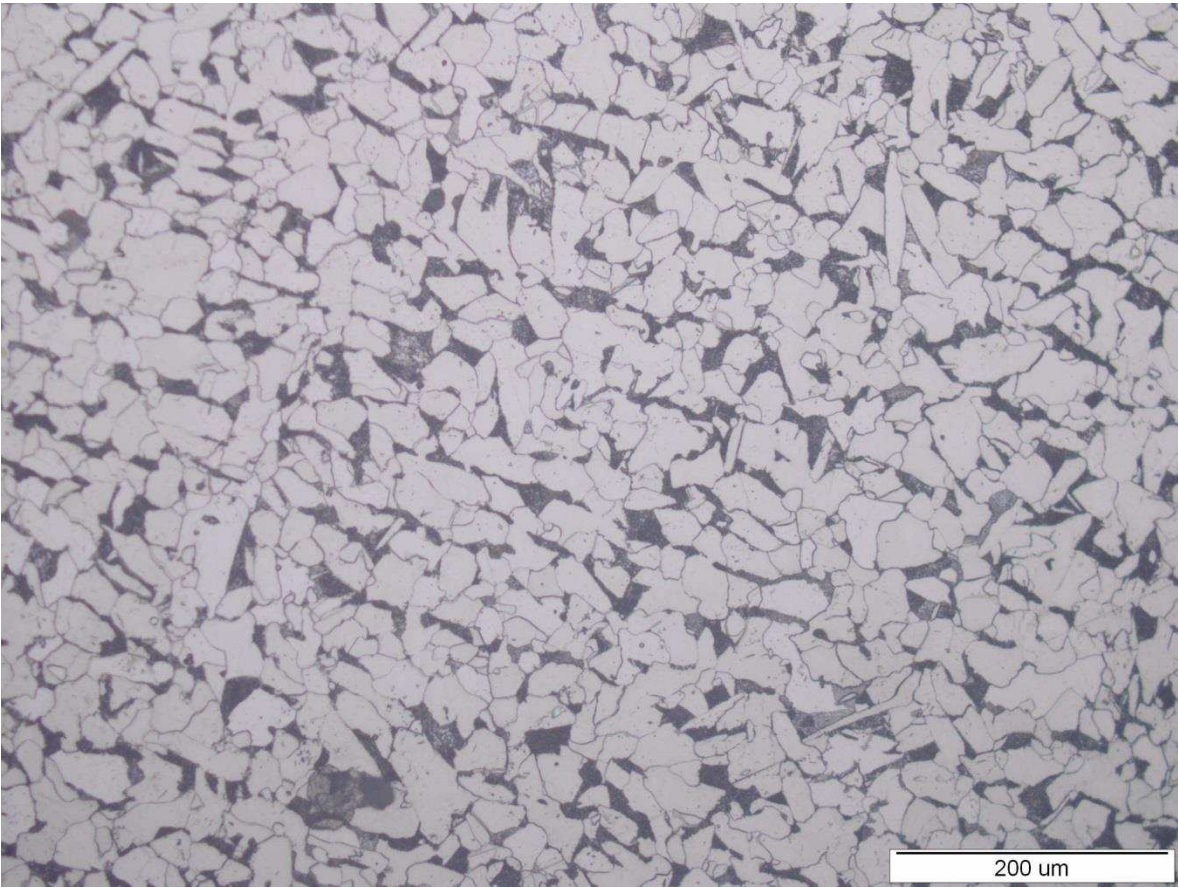


Figure 7

Table 1

Temperature (°C)	Modulus of elasticity $E_{y,\theta}$ (GPa)	Yield strength $f_{0.2,\theta}$ (MPa)	Ultimate strength $f_{u,\theta}$ (MPa)	ϵ_t (%)
20	204.7	287.5	488.0	26.2
100	204.6	266.4	480.7	35.0
200	192.2	288.5	641.0	16.8
300	172.8	214.7	509.9	22.3
400	164.9	239.3	370.4	16.5
450	162.0	203.3	300.1	17.3
500	142.7	174.7	222.6	27.1
550	135.0	134.0	158.9	18.2
600	130.0	97.6	106.6	41.4

Table 2

Temperature (°C)	Stationary creep test parameters			
	Stress σ (MPa)	$\sigma/f_{0.2,0}$	Time of the occurrence of secondary phase (min)	Time of the occurrence of tertiary phase (min)
400	167.5	0.7	-	-
	191.0	0.8	-	-
	215.0	0.9	-	-
450	151.75	0.75	200	630
500	78.6	0.45	100	315
	87.4	0.5	70	240
	104.8	0.6	30	95
	139.8	0.8	9	30
550	87.2	0.65	10	30
600	24.4	0.25	195	450
	29.3	0.30	100	280
	63.4	0.65	3	9
	73.2	0.75	2	4

Table 3

Temperature (°C)	Reduction factors						
	Exp $f_{y,\theta}/f_{y,20} - 2\%$	EC3 [1] $f_{y,\theta}/f_{y,20} - 2\%$	Exp $f_{0.2,\theta}/f_{0.2}$	<i>Brnić et al.</i> [9] $f_{0.2,\theta}/f_{0.2}$	Exp $E_{y,\theta}/E_{y,20}$	EC3 [1] $E_{y,\theta}/E_{y,20}$	<i>Brnić et al.</i> [9] $E_{y,\theta}/E_{y,20}$
100	0.98	1.0	0.93	0.96	1.0	1.0	0.97
200	1.17	1.0	1.00	0.83	0.94	0.9	0.92
300	0.99	1.0	0.75	0.66	0.84	0.8	0.87
400	0.93	1.0	0.83	0.59	0.81	0.7	0.83
500	0.62	0.78	0.66	0.44	0.70	0.6	0.73
600	0.31	0.47	0.34	0.22	0.64	0.31	0.48

Table 4

Study	C	Si	Mn	P	S	Ni	Cr	Mo	Cu	Al	Rest
S275 – Exp	0.186	0.245	0.653	0.010	0.005	0.167	0.078	0.028	0.319	0.011	98.30
S275 [9]	0.08	0.22	0.57	0.025	0.017	0.14	0.10	0.02	0.50	0.002	98.33
43A [2]	0.24	0.032	0.96	0.038	0.022	0.017	0.013	0.005	0.019	0.002	98.65
A36 [16,19]	0.19	0.09	0.71	0.007	0.03	-	-	-	-	-	-
S355 [22]	0.163	0.22	1.44	0.007	0.001	0.14	0.19	0.002	0.19	0.031	97.62

Table 5

Temperature (°C)	Coefficient	Stress level (MPa)			
		167.5 (0.7f _{0.2,0})	191.0 (0.8f _{0.2,0})	215.0 (0.9f _{0.2,0})	
400	a	0.06431	0.09918	0.25200	
	b	0.12840	0.12700	0.15150	
	c	0.10165	0.11591	0.13047	
	e	-	-	-	
	f	-	-	-	
		78.6 (0.45f _{0.2,0})	87.4 (0.5f _{0.2,0})	104.8 (0.6f _{0.2,0})	139.8 (0.8f _{0.2,0})
500	a	3.788E-04	0.01956	0.00548	0.25720
	b	0.83560	0.42470	1.10100	0.76090
	c	0.05509	0.06126	0.07345	0.09796
	e	6.920E-07	2.464E-06	4.567E-08	2.324E-05
	f	1.90100	1.94600	2.90200	2.89700
		24.4 (0.25f _{0.2,0})	29.3 (0.30f _{0.2,0})	63.4 (0.65f _{0.2,0})	73.2 (0.75f _{0.2,0})
600	a	2.595E-05	3.967E-04	0.05409	0.37110
	b	1.13400	0.87670	1.13800	1.28200
	c	0.01877	0.02254	0.04881	0.05631
	e	5.984E-14	7.687E-09	8.853E-05	1.325E-06
	f	0.57650	2.42500	2.71600	5.51700